2013

Microscopic distribution of extended defects and blockage of threading dislocations by stacking faults in semipolar (1101)(1101)()(1101)() GaN revealed from spatially resolved luminescence

S. Okur
Virginia Commonwealth University, okurs@vcu.edu

S. Metzner
Institute of Experimental Physics

N. Izyumskaya
Virginia Commonwealth University, nizioumskaia@vcu.edu

See next page for additional authors

Okur, S., Metzner, S., Izyumskaya, N., et al., Microscopic distribution of extended defects and blockage of threading dislocations by stacking faults in semipolar (1101)(1101)()(1101)() GaN revealed from spatially resolved luminescence. Applied Physics Letters, 103, 211908 (2013).

Microscopic distribution of extended defects and blockage of threading dislocations by stacking faults in semipolar $(1\bar{1}01)$ GaN revealed from spatially resolved luminescence

S. Okur,[1] S. Metzner,[2] N. Izyumskaya,[1] F. Zhang,[1] V. Avrutin,[1] C. Karbaum,[2] F. Bertram,[2] J. Christen,[2] H. Morkoç,[1] and Ü. Özgür[1,a)]
[1]*Department of Electrical and Computer Engineering, Virginia Commonwealth University, Richmond, Virginia 23284, USA*
[2]*Institute of Experimental Physics, Otto-von-Guericke-University Magdeburg, Magdeburg D-39106, Germany*

(Received 15 August 2013; accepted 9 October 2013; published online 21 November 2013)

Spatial distribution of extended defects in semipolar $(1\bar{1}01)$-oriented GaN layers grown on patterned (001) Si substrates with striped grooves of varying width was investigated by optical means only using near-field scanning optical microscopy (NSOM) and cathodoluminescence (CL). A high density of basal and prismatic stacking faults was observed in the c$^-$ wings, and the threading dislocations in c+ wings, which appear as dark patterns in the NSOM and CL images, were found to bend toward the surface during the initial stages of growth. In the case when growing c+ front of GaN made contact with the SiO_2 masking layer during growth, stacking faults were found to form also in the c+ wings. These additional stacking faults effectively blocked propagation of dislocations along the c+ direction, resulting in high quality stripes virtually free of defects. As revealed by optical means only without the need for any structural investigation, such control over the threading dislocation density using select growth geometries is potentially advantageous for improving semipolar $(1\bar{1}01)$GaN. © *2013 AIP Publishing LLC*. [http://dx.doi.org/10.1063/1.4826579]

A vast majority of GaN-based light emitting diodes (LEDs) and laser diodes (LDs) employ polar (0001) GaN orientation due to its well-established technology. However, large spontaneous and piezoelectric polarization fields present along the polar [0001] direction reduce the radiative recombination efficiency due to separation of electron and hole wavefunctions in wide active regions, and result in injection-dependent emission wavelength and efficiency. To resolve or mitigate these problems, nonpolar or semipolar GaN orientations[1,2] on mainly low-cost foreign substrates such as Si[3,4] and sapphire[5,6] have been considered. Silicon substrate is of particular interest due to its availability in large sizes and good thermal and electrical conductivities.[7,8] Semipolar $(1\bar{1}01)$ InGaN LEDs grown on patterned Si substrates have been shown to exhibit reduced efficiency loss[9] compared to their polar counterparts on sapphire and promisingly high internal quantum efficiency.[10] However, further reduction of point and extended defects such as threading dislocations (TDs) and stacking faults (SFs) is warranted to take full advantage of different semipolar orientations of GaN.[4,11,12] In this work, spatially and spectrally resolved near-field scanning optical microscopy (NSOM) and cathodoluminescence (CL) methods were applied to investigate the effect of growth geometry, specifically that of the stripe pattern, on defect distributions, and consequently the optical quality of semipolar $(1\bar{1}01)$ GaN structures on Si substrates.

Semipolar $(1\bar{1}01)$ GaN layers were grown on patterned Si by metal-organic chemical vapor deposition (MOCVD) using trimethylgallium (TMGa) and NH_3 as sources of Ga and NH_3 with mass flow rates of 8 sccm and 3500 sccm, respectively, at a chamber pressure of 200 Torr and a temperature of 1040 °C. Si(001) substrates offcut by 7° toward the Si⟨110⟩ direction were patterned to form grooves of either 3 or 10 μm width, from here and on referred to as the narrow- or wide-groove patterns, respectively, separated by 3 μm terraces. The patterning procedure and initiation of GaN growth on the Si(111) facets exposed within the grooves have been described elsewhere.[8,13] It should be noted that the wide groove pattern (3 μm × 10 μm) does not allow physical contact of the growing GaN stripe with the opposing Si(111) facet, whereas the narrow groove pattern (3 μm × 3 μm) promotes such physical contact and results in a fully coalesced layer for the growth time employed as evidenced from the cross-sectional scanning electron microscopy (SEM) images in Figure 1. Spatial distribution of extended defects in $(1\bar{1}01)$ GaN samples with different size patterns was studied at room temperature using a Cryoview 2000 NSOM system (Nanonics Imaging Ltd) and at 5.8 K using a CL system built around a JEOL 6400 scanning electron microscope.[14] For NSOM measurements, HeCd laser (325 nm wavelength) excitation through a Cr-Al coated optical fiber probe with a 100 nm aperture was used.[15]

As seen from Figure 1, the growth in the $[000\bar{1}]$ GaN direction (c− wing) is very limited due to the growth geometry. For simplicity, the part of the GaN stripe adjacent to the c− wing will hereafter be referred to as c− side, and the remaining part, as c+ side, as indicated in Figure 1. The NSOM and CL characterization data for the wide-groove pattern sample are summarized in Figure 2. The atomic force microscopy (AFM) image in Figure 2(a) and the corresponding NSOM near-band edge emission (NBE) intensity map (integrated between 350 and 370 nm) in Figure 2(b) for the

a)Electronic mail: uozgur@vcu.edu

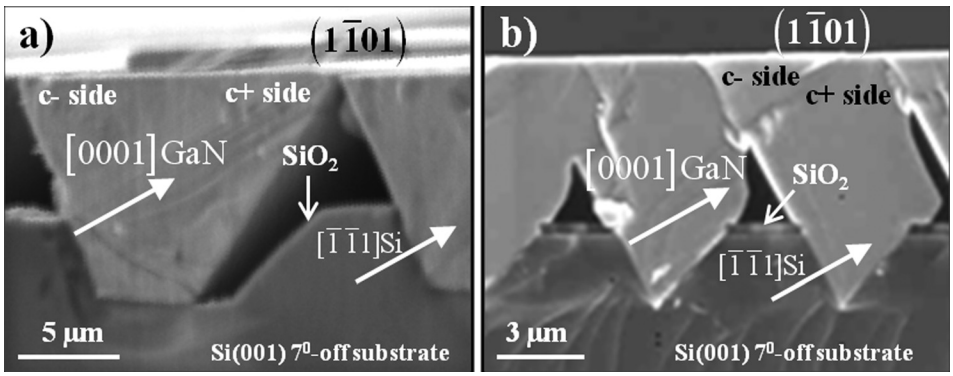

FIG. 1. Cross-sectional SEM images for (a) wide- and (b) narrow-groove pattern (1$\bar{1}$01) GaN samples.

wide-groove pattern sample show that NBE originates mainly from the c+ sides of the stripes. Figure 2(c) shows the steady-state PL spectra for the wide- and narrow-groove pattern samples collected at 15 K and 295 K. At 15 K, the intensities of the donor-bound exciton (D^0X) emission for both samples are comparable to that for a state-of-the-art polar GaN template (~10 μm thick) grown on sapphire using *in situ* epitaxial lateral overgrowth (ELO) with a SiN_x nano-network mask.[16] Compared to the c-plane GaN reference sample, the relatively higher intensities of the basal stacking fault (BSF) and prismatic stacking fault (PSF)[17] related PL peaks (3.416 eV and 3.336 eV, respectively, for the narrow-groove pattern sample) are indicative of a larger density of stacking faults in the semipolar (1$\bar{1}$01) GaN samples. The presence of a high density of defects is evident also from the rapid decrease of the internal quantum efficiency (IQE) from the assumed 100% at 15 K to 4% at 100 K and 1% at room temperature for the wide-groove pattern sample. The well-known optical signatures of these defects are the key to characterization of their distribution in the samples explored here.

The distinction between the c+ and c− sides in terms of the defect densities and the optical quality deduced from NSOM data is confirmed from the SEM and the corresponding 5.8 K CL intensity (integrated between 350 and 380 nm) and CL peak wavelength images shown in Figures 2(d)–2(f), respectively. The CL NBE (~3.47 eV or ~357 nm) mainly originates from the c+ sides, and the overall emission from the c− sides is significantly weaker. In accord with the low temperature PL spectra [Figure 2(c)], the BSF and PSF CL peaks were observed mainly at 362–366 nm (~3.423–3.386 eV) and around 374 nm (~3.314 eV), respectively. The

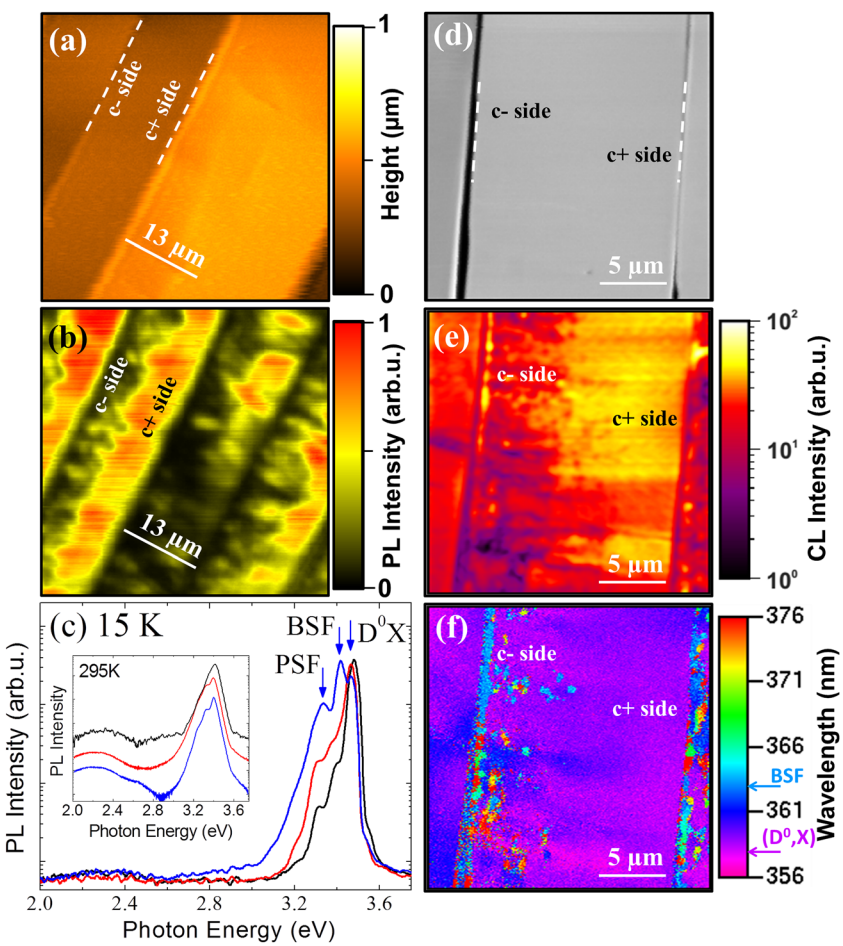

FIG. 2. Top-view (a) AFM and (b) the corresponding room temperature near-band edge emission (integrated between 350–370 nm) NSOM images, (c) 15 K and room temperature PL spectra (red), (d) SEM, and the corresponding 5.8 K (e) CL intensity (integrated between 350 and 380 nm), and (f) CL peak wavelength images of the wide-groove pattern (1$\bar{1}$01) GaN sample. In (c), the PL spectra for the narrow-groove pattern (1$\bar{1}$01) GaN sample (blue) and a c-plane GaN reference sample (black) are also shown.

slight differences in the PL and CL peak positions are likely due to local strain variations and the differences in excitation density. The CL peak wavelength image of Figure 2(f) also indicates that these stacking faults are mostly distributed over the c– sides while their density peaks in the c– wings of the stripes. It should be noted that the emission from BSFs is suppressed at room temperature due to weak binding energy of carriers to the BSFs.[18] Additional nonradiative centers due to TDs and associated point defects are also manifested as dark regions in NSOM PL and CL images. The dark patterns elongated normal to the stripes correspond to TDs that originate from the Si interface and reach the $(1\bar{1}01)$GaN surface mainly in the c– sides.

In order to further understand the distribution of TDs in the wide-groove pattern sample, cross-sectional CL measurements were performed. As seen in Figure 3(a), CL intensity diminishes at the GaN/Si interface where the growth initiates, and therefore, a high density of TDs exists. During the initial stages of growth, the TDs propagate along the c+ direction. However, as the growth proceeds, the TDs which propagate in the vicinity of $\{1\bar{1}01\}$ growth fronts bend toward them under the action of image forces[19] as schematically shown in Figure 3(b). Similar observations related to the TD bending were made by Murase *et al.*[20] in CL measurements of a semipolar $(11\bar{2}2)$ GaN template grown on a patterned (113) Si substrate. Gradeèaka *et al.*[19] demonstrated for epitaxial lateral overgrowth of c-plane GaN that a significant portion of the TDs bend by 90° (depending on the type of dislocation and the associated Burger's vector, intermediate bending angles of ~45° and ~60° have also been observed[19,21]). and then propagate in the basal plane, i.e., in the direction perpendicular to major progressing growth front for our geometry, as illustrated in Figure 3(b). The rest of TDs propagate in the c+ direction perpendicular to the growing (0001) front and terminate at the lower $\{1\bar{1}01\}$ facets. As a result, a relatively narrow slice of the defective material (referred to here as the c– side) forms adjacent to the c– wing of the stripe (appearing as a dark region on the top-view and cross-sectional CL and NSOM images shown in Figures 2 and 3). For the growth geometry employed here, a high quality region free of TDs and exhibiting high luminescence intensity is achieved on the c+ sides of the stripes as clearly observed in Figure 3(a).

As evident from the cross-sectional CL image of Figure 3(a), there is some variation in the CL intensity from the adjacent stripe; however, the general trends described above have been observed in other CL images collected across the sample. These variations may be explained by slight disparity in BSF and TD distributions for different $\{1\bar{1}01\}$ GaN stripes. It should also be noted that the absence of NBE and BSF emission from the GaN/Si interface is indicative of a high density of TDs and suggests that any BSFs present in these regions are of the short variety terminated by partial dislocations at the ends, which are not optically active.[22]

The distribution of defects is quite different in the narrow-groove pattern sample as evidenced from the NSOM and CL images in Figure 4. The AFM (not shown) and SEM [Figure 4(a)] images indicate a relatively smooth surface achieved upon coalescence. The BSF and PSF densities are significantly higher in the narrow-groove pattern sample compared to that with the wide-grooves as evidenced from the higher intensities of the corresponding PL lines [see Figure 2(c)]. Moreover, the narrow-groove pattern sample exhibits nearly 30 times lower NBE at room temperature than the wide-groove pattern sample due to a significantly higher density of extended defects inclusive of threading dislocations and the associated point defects.

The regions with high density of BSFs are manifested as high brightness rows in plan-view [Figure 4(b)] and cross-sectional [Figure 5(a)] CL intensity images. The CL peak wavelength images in Figure 4(c) and Figure 5(b) confirm the presence of BSFs (~364 nm emission) in the c– wings as well as within the c+ wings. As shown in our earlier study,[13] additional BSF rows were formed where the growing c+ fronts of GaN made contact with the SiO_2 masking layer on the opposite side of the groove in the Si substrate (Figure 5). Concentration of strain near the region in contact with SiO_2 and/or oxygen and/or silicon out-diffusion from SiO_2 followed by surface migration of the species have been proposed as possible causes, and further microscopic studies are warranted to identify their origin.[13] These additional BSF rows within the c+ sides are found to play a critical role in improving the material quality in the narrow-groove pattern $(1\bar{1}01)$ GaN sample. As evident from the plan-view CL intensity image of Figure 4(b) the TDs, manifested as dark spotty patterns along the *c* direction, are blocked by the additional BSF rows. It is also clear from the cross-sectional CL intensity [Figure 5(a)] and CL peak wavelength [Figure 5(b)] images that c- sides of the additional BSF rows exhibit dark contrast due to a high density of TDs compared to the c+ sides. Some of the TDs initially propagating along the *c* direction are bent into the basal plane with further growth as in the wide-groove pattern sample, and those continuing along the *c* direction are terminated if they encounter an additional BSF row. This is illustrated in the schematic of Figure 5(c). As a result of this interaction between the TDs and the BSFs, the regions between the two BSF rows are virtually free of TDs [see the bright regions between two BSF

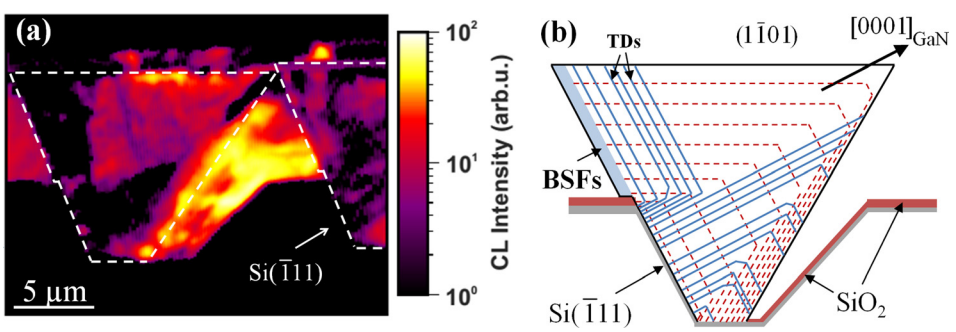

FIG. 3. (a) Cross-sectional integrated CL intensity image (350–380 nm) for the wide-groove pattern sample. The dashed lines represent GaN growth boundaries. (b) Cross-sectional schematic of GaN growth from Si(1̄11) sidewall showing TD propagation (blue lines) and the growth fronts (dashed lines). Note that propagation of the bottom $(1\bar{1}01)$ front is the slowest because of limited material supply.

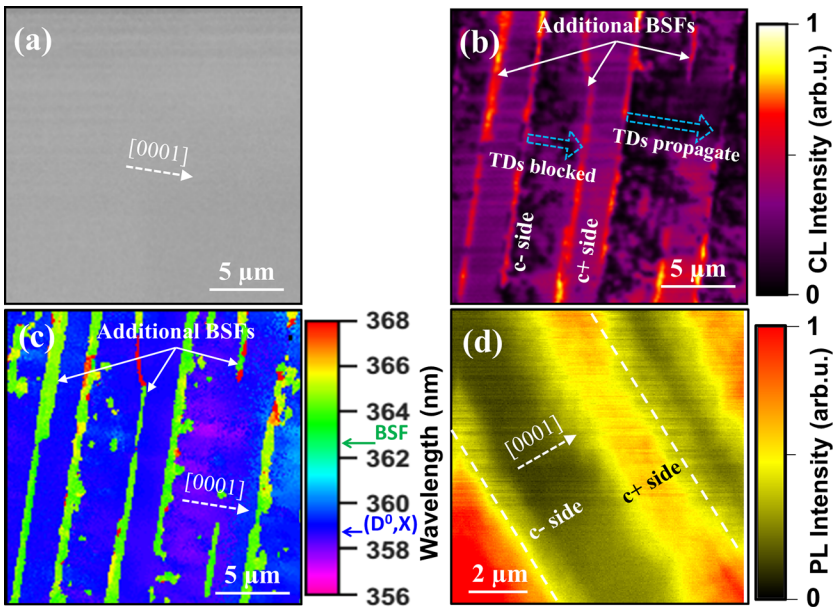

FIG. 4. Plan-view (a) SEM and the corresponding 5.8 K (b) CL intensity (350–380 nm) and (c) CL peak wavelength images, and (d) room temperature near-band edge emission NSOM image of the narrow-groove pattern $(1\bar{1}01)$ GaN sample. The projection of the c-axis is also indicated on the images.

rows in Figure 4(b) and Figure 5(a)]. This is also confirmed by the NSOM NBE intensity image of Figure 4(d), which shows periodic high brightness stripes representing the high quality regions between the two BSF rows. Although the detailed mechanism of TD-BSF interaction requires further investigations, we can cautiously speculate that the TDs bend at the additional BSF row interface, which is in fact a boundary between the hexagonal and cubic phase materials, and turn into misfit dislocations extending towards the top and the bottom $(1\bar{1}01)$ surfaces. The effective blocking of TDs by additional BSFs in the narrow-groove pattern sample can be very beneficial to further reduce the TD density without the need for a two-step selective growth technique.[20]

In summary, semipolar $(1\bar{1}01)$ GaN layers grown on Si(001) 7° off cut substrates with 3 μm and 10 μm wide groove patterns were studied by steady-state PL and spatially resolved NSOM and CL with emphasis on the distribution of defects and their effects on the optical quality. The PL from the near surface c+ sides of the semipolar $(1\bar{1}01)$ GaN layers are found to be mainly dominated by the strong near bandedge emission; however, emission from the c− sides is substantially weaker due to high density of threading dislocations and stacking faults. By entirely optical means, without the need for any structural microscopy analysis, it was revealed that some TDs bend toward the surface. Additional stacking faults formed in the narrow-groove pattern sample when the growing c+ fronts made contact with the SiO_2 masking layer were found to block TD propagation along the c+ direction. These results indicate that, for proper Si(001) substrate patterning geometry, high quality $(1\bar{1}01)$ GaN free from extended defects can be obtained using a single ELO step.

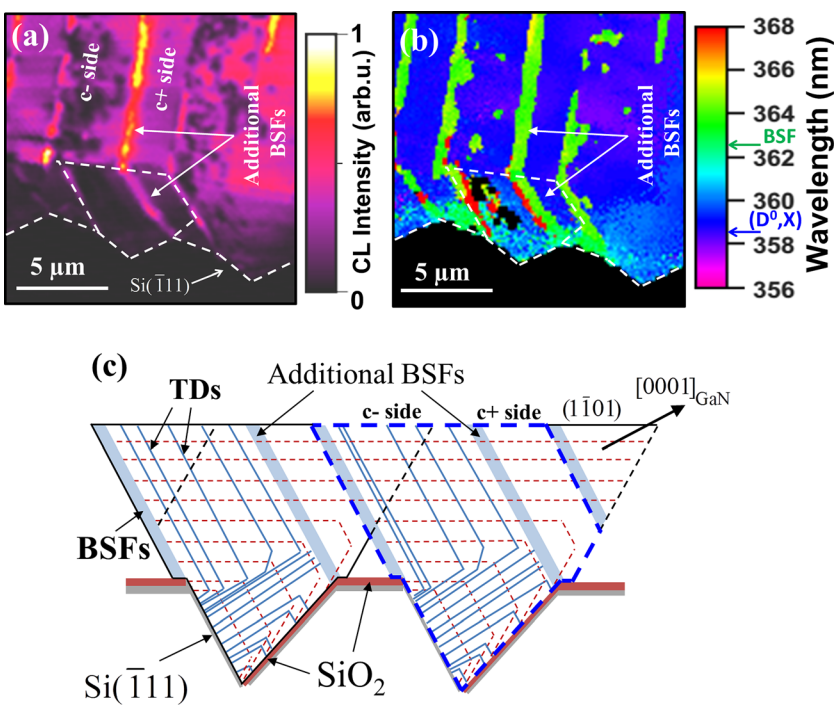

FIG. 5. Cross-sectional (a) integrated CL intensity (350–380 nm) and (b) CL peak wavelength images for the narrow-groove pattern sample $(1\bar{1}01)$ GaN sample. The solid and dashed lines indicate the Si substrate surface and the GaN stripe cross section, respectively. (c) Cross-sectional schematic of GaN growth from Si$(\bar{1}11)$ sidewall showing threading dislocation propagation (blue solid lines) and the growth fronts (red dashed lines).

The work at VCU was funded by the National Science Foundation (projects DMR # 0907096 and DMR #1210282 under direction of Dr. C. Ying). The work at Magdeburg University is funded by the German Research Foundation DFG in the frame of the research unit FOR 957 "PolarCoN."

[1]H. Morkoç, *Handbook of Nitride Semiconductors and Devices* (Wiley-VCH, Weinheim, 2008), Vol. 2.
[2]T. Paskova, *Nitrides with Nonpolar Surfaces: Growth, Properties, and Devices* (Wiley-VCH, Weinheim, 2008).
[3]A. Dadgar, R. Ravash, P. Veit, G. Schmidt, M. Muller, A. Dempewolf, F. Bertram, M. Wieneke, J. Christen, and A. Krost, Appl. Phys. Lett. **99**, 021905 (2011).
[4]N. Sawaki, T. Hikosaka, N. Koide, S. Tanaka, Y. Honda, and M. Yamaguchi, J. Cryst. Growth **311**, 2867 (2009).
[5]T. Sasaki and S. Zembutsu, J. Appl. Phys. **61**, 2533–2540 (1987).
[6]X. Ni, Y. Fu, Y. T. Moon, N. Biyikli, and H. Morkoç, J. Cryst. Growth **290**, 166 (2006).
[7]N. Sawaki and Y. Honda, Sci. China, Ser. E Technol. Sci. **54**, 38 (2011).
[8]N. Izyumskaya, S. J. Liu, V. Avrutin, S. Okur, F. Zhang, Ü. Özgür, S. Metzner, C. Karbaum, F. Bertram, J. Christen, D. J. Smith, and H. Morkoç, Proc. SPIE **8262**, 826224 (2012).
[9]C.-H. Chiu, D.-W. Lin, C.-C. Lin, Z.-Y. Li, W.-T. Chang, H.-W. Hsu, H.-C. Kuo, T.-C. Lu, S.-C. Wang, W.-T. Liao, T. Tanikawa, Y. Honda, M. Yamaguchi, and N. Sawaki, Appl. Phys. Express **4**, 012105 (2011).
[10]T. Murase, T. Tanikawa, Y. Honda, M. Yamaguchi, and H. Amano, Phys. Status Solidi C **8**, 2160 (2011).
[11]Y. Honda, N. Kameshiro, M. Yamaguchi, and N. Sawaki, J. Cryst. Growth **242**, 82 (2002).
[12]T. Hikosaka, T. Narita, Y. Honda, M. Yamaguchi, and N. Sawaki, Appl. Phys. Lett. **84**, 4717 (2004).
[13]N. Izyumskaya, F. Zhang, S. Okur, T. Selden, V. Avrutin, Ü. Özgür, S. Metzner, C. Karbaum, F. Bertram, J. Christen, and H. Morkoç, J. Appl. Phys. **114**, 113502 (2013).
[14]F. Bertram, T. Riemann, J. Christen, A. Kaschner, A. Hoffmann, C. Thomsen, K. Hiramatsu, T. Shibata, and N. Sawaki, Appl. Phys. Lett. **74**, 359 (1999).
[15]Ü. Özgür, X. Ni, Y. Fu, H. Morkoç, and H. O. Everitt, Appl. Phys. Lett. **89**, 262117 (2006).
[16]J. Xie, Ü. Özgür, Yi Fu, X. Ni, H. Morkoç, C. K. Inoki, T. S. Kuan, J. V. Foreman, and H. O. Everitt, Appl. Phys. Lett. **90**, 41107 (2007).
[17]R. Liu, A. Bell, F. A. Ponce, C. Q. Chen, J. W. Yang, and M. A. Khan, Appl. Phys. Lett. **86**, 021908 (2005).
[18]P. Corfdir, P. Lefebvre, J. Levrat, A. Dussaigne, J.-D. Ganière, D Martin, J. Ristić, T. Zhu, N. Grandjean, and B. Deveaud-Plédran, J. Appl. Phys. **105**, 043102 (2009).
[19]S. Gradeèaka, P. Stadelmann, V. Wagner, and M. Ilegems, Appl. Phys. Lett. **85**, 4648 (2004).
[20]T. Murase, T. Tanikawa, Y. Honda, M. Yamaguchi, H. Amano, and N. Sawaki, Jpn. J. Appl. Phys., Part 1 **50**, 01AD04 (2011).
[21]P. Gibart, Rep. Prog. Phys. **67**, 667 (2004).
[22]Z. H. Wu, A. M. Fischer, F. A. Ponce, B. Bastek, J. Christen, T. Wernicke, M. Weyers, and M. Kneissl, Appl. Phys. Lett. **92**, 171904 (2008).